THE EFFECTS OF ARGON PRESSURE ON THE RESONANCE LINE OF STRONTIUM*,**

By Shang Yi Chen and Shih Yuan Wang

Physics Department, University of Oregon, Eugene***

(Received April 24, 1978)

The shape, half-width and shift of the resonance line of strontium at 4607 Å were measured under various pressures of argon ranged from 10 PSI (at 474°C) to 2,370 PSI (at 564°C). The semi-empirical force constants of the interatomic potential of Lennard-Jones (6–12) form were obtained ($\Delta C_6 = 1.02\times10^{-57}$ erg cm^6 and $\Delta C_{12} = 0.86\times10^{-99}$ erg cm^{12}) and other physical constants of the difference potential curve were determined. The results furnish a representative sample of the foreign gas effects on a spectral line due to argon.

1. *Introduction*

The broadening of the strontium resonance line (5^1S-5^1P) at λ4607 was studied by Farr and Hindmarsh [1] at pressures less than one atmosphere of argon. Their interest was limited to this low pressure region where the line shape was Lorentzian. The purpose of the present work is to provide accurate measurements of the shape, shift, and broadening of the strontium resonance line under very well defined conditions of temperature and pressure of argon for pressures over a hundred fold of those previously studied. A comparison is made between the results of the present work and those obtained for Ca 4227 in Ar [2].

2. *Experimental*

The schematic diagram in Fig. 1 may serve to supplement what was reported before [2]. Reference lines for shift measurement were added to recording paper by focusing light from a xenon or an argon discharge tube upon the spectrograph slit. The absorption column and the furnace assembly, as shown in Fig. 2, were attached to one endplate of the pressure cell (as shown) so that they were held within the cell in optical alignment and were thermally insulated from the cell walls. The pressure cell is a steel cylinder 59 cm

* Dedicated to Professor Aleksander Jabłoński on the occasion of his 80th birthday.

** Research sponsored by the National Science Foundation of the USA.

*** Address: Physics Department, University of Oregon, Eugene, Oregon 97403, USA.

long and 33 cm O. D. with 11 cm wall thickness and was tested to stand gas pressures up to 3,400 atmospheres. The absorption column is a steel tube 1.0 cm I. D. and 5.0 cm in length. Two sapphire windows spaced 1.5 cm apart by a sleeve were used on each side of

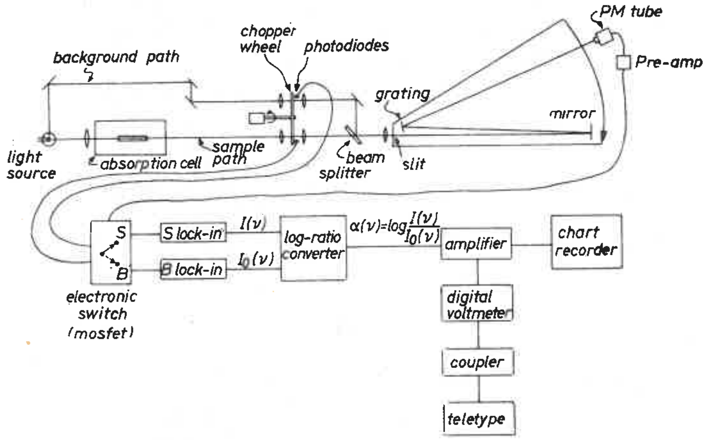

Fig. 1. Experimental arrangement

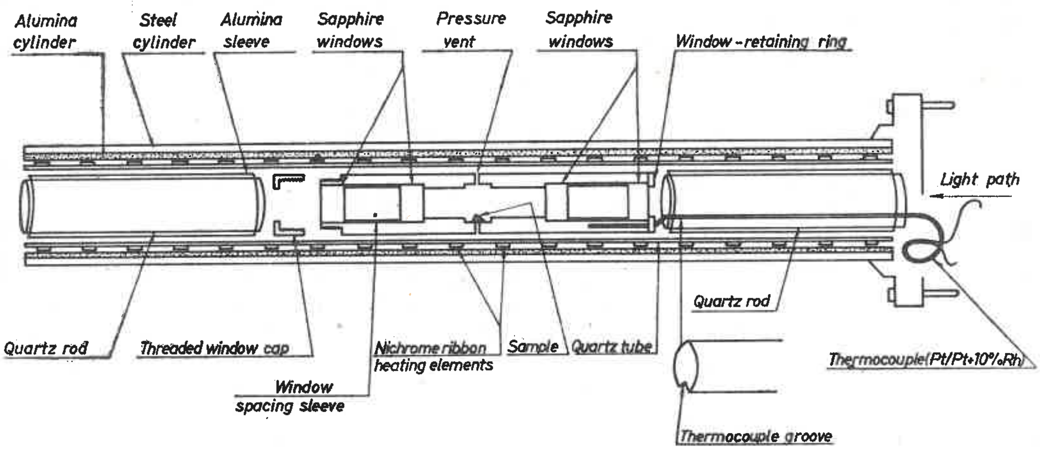

Fig. 2. The absorption column and the furnace

the absorption column. Also on each side a 10 cm long clear quartz rod was placed between the absorption column and the quartz window on the end plate to avoid gas convections in the light path.

The temperature of the absorption column was maintained to within $\pm 1/2$°C by a Leeds and Northrup controller. The pressure readings were taken from 16″ dial Heise gauges which were accurate to 1/2%. An EMI 6256 ŜA photomultiplier tube with "S" (Q) response was used. The tube was housed in a refrigerated chamber with a cooling period of 8 hours at -74°C, and had a no-dew ring to prevent condensation on the outer window. The detection system (shown in Fig. 1) employed a phase-sensitive detector with dual beam design and log-ratio output. The sample beam (which traversed the absorption column) and the reference beam (which traversed the ambient atmosphere) were presented alternatively to a 30-μ entrance slit of the spectrograph at 450-hz rate by means of a chopper wheel. The photomultiplier tube mounted behind a 30-μ exit slit, scanned the spectrum. Its output was demodulated by a FET switch (synchronized to the chopper wheel) and detected by two lock-in amplifiers. Their outputs were fed to a log--ratio op-amp module whose output is proportional to the log of its two inputs. The signal which directly represented the absorption coefficient was displayed on a chart recorder or digitized on a paper tape for computer data analyses. Experimental points on the plots were usually the average values of several determinations.

3. *Results and discussions*

A. The profiles

The resonance line of Sr in argon (hereafter denoted by Sr(1)/Ar) displayed a Lorentzian shape when the relative density (hereafter denoted by r. d.) of Ar was below one, but deviated appreciably at high densities. Fig. 3 gives the line profiles under various pressures

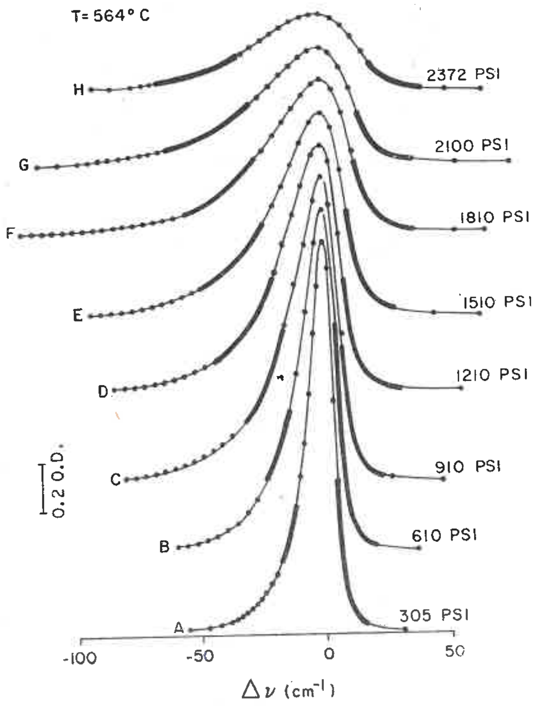

Fig. 3. Profiles of Sr 4607 under various pressures of argon (T = 564°C). The ordinate is optical density (the indicated vertical scale is for O.D. = 0.2). $\Delta\nu$ is the frequency distance from the line peak in cm^{-1}. The (–3/2) power relationship portion of the red wings and the (–7/3) power relationship portion of the violet wings are indicated by bold lines

of argon for which the r. d.'s ranged from 6.72 to 50.22. The ordinate is the intensity of absorption expressed as optical density, O. D.; and $\Delta\nu$ is the frequency distance measured from the line peak in cm^{-1}. They are lined up at the peak frequencies and displaced vertically from each other to avoid confusion. It is clear that the lines were broadened asymmetrically towards red showing a predominance of van der Waals forces between the Sr and Ar.

A plot of ln (I) vs ln ($\Delta\nu$) measured from the *red* wing is given in Fig. 4. For comparison, a line having a slope of $-3/2$ is shown. The plots show that Kuhn's ($-3/2$) power relationship [3] held only for a limited region of $\Delta\nu$. These ($-3/2$) power regions are indicated by bold lines in Fig. 3 and are also tabulated in Table I. The result shows that as the r. d. of Ar increases, the regions moved towards the larger ($-\Delta\nu$) as anticipated.

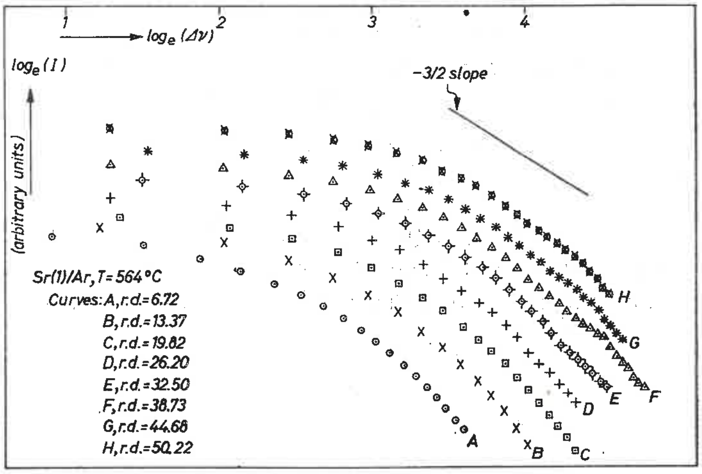

Fig. 4. Plot of ln (I) vs ln($\Delta\nu$) for the red wings of Sr(1)/Ar

TABLE I

The $-3/2$ power relationship portions of the red wings and the $-7/3$ power relationship portions of the violet wings of Sr(1)/Ar

Profile	T (°C)	P (PSI)	r.d of Ar	Red wings: $-3/2$-power-portion (cm^{-1})	Red wings: Interval (cm^{-1})	Violet wings: $-7/3$-power-portion (cm^{-1})	Violet wings: Interval (cm^{-1})
A	564	305	6.72	12.6—18.5	5.90	4.5—16.4	11.9
B	564	610	13.37	14.9—24.5	9.6	5.3—20.1	14.8
C	564	910	19.82	16.4—31.8	15.4	6.8—21.1	14.3
D	564	1210	26.20	20.1—40.4	20.3	8.7—30.0	21.3
E	564	1510	32.50	24.5—49.4	24.9	10.8—30.0	19.2
F	564	1810	38.73	27.1—54.5	27.4	13.2—36.6	23.4
G	564	2100	44.68	29.9—60.3	30.4	16.1—36.6	20.5
H	564	2372	50.22	33.1—66.6	33.5	19.3—40.4	21.1

If the same procedures are carried out for the *violet* wings, one obtains Fig. 5. These curves are reasonably linear in their central regions with slopes around $-(7/3)$. The part of the wings which exhibited a $-(7/3)$ power relation as predicted by Lindholm's theory [4]

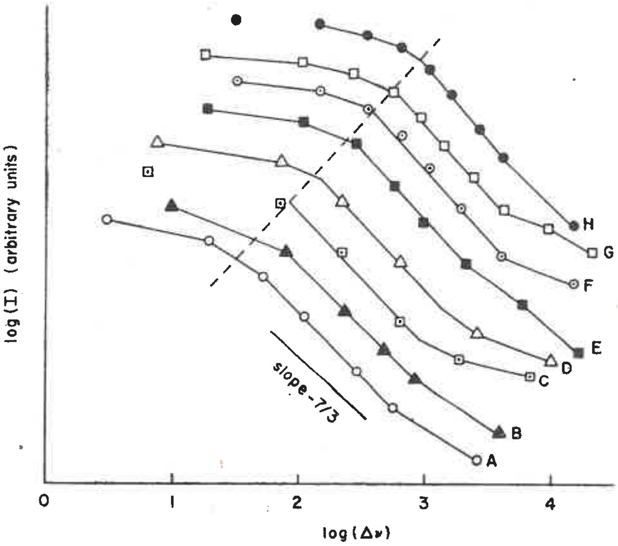

Fig. 5. Plot of $\ln(I)$ vs $\ln(\Delta\nu)$ for the violet wings of Sr(1)/Ar

is indicated in Fig. 3 by another set of bold lines on the violet wings, and is also tabulated in Table I. These experimental wings are also consistent with Anderson and Talman [5] general pressure broadening theory for r^{-6} interatomic potential and low r. d.

B. The half-width, shift and asymmetry

Since the vapor pressure of Sr is low, one needs to heat the absorption column to above 500°C for an absorption column of length 5.0 cm to obtain good profile measurements. At 590°C, the Doppler half-width [6] for Sr is approximately 0.05 cm^{-1} which is

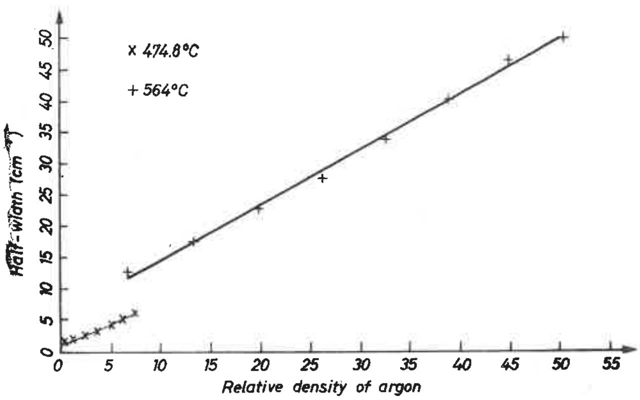

Fig. 6. Plot of half-width vs r. d. of argon

negligible. Fig. 6 is a linear fit of the plot of half-width vs r. d. for r. d.'s ranging from 0.45 to 7.4 (at 474.8°C) the plot yield a slope of 0.64 cm^{-1}/r. d. Hindmarsh's value was $2\times 1.30\times 10^{-20} cm^{-1}$ (atom $cm^{-3})^{-1}$ or 0.70 cm^{-1}/r. d. at 407°C. The value for Ca (1)/Ar is 0.67 cm^{-1}/r. d. at 556°C. The agreement is excellent.

For r. d.'s ranging from 6.72 to 50.22 (at 564°C) the slope is 0.88 cm^{-1}/r. d. The corresponding data for Ca(−1)/Ar is 1.0 cm^{-1}/r. d. at 638°C. It may be noted that the half-width is temperature dependent.

The shift plotted against the r. d. of Ar is given in Fig. 7. Since a "red" shift is treated as negative $\Delta\nu$, Fig. 7 produced a negative slope. The points are fitted by a fourth-degree polynomial. It is seen that the linearity of the plot was not followed over the whole range

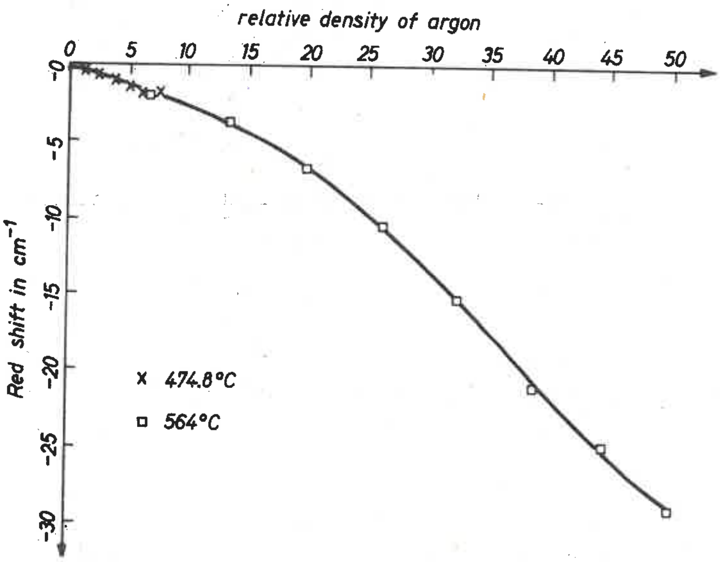

Fig. 7. Plot of shift vs r.d. of argon

of r. d. Fig. 7 may be described as having four regions. The first region is linear, which occurred at low r. d.'s (r. d. from less than 0.1 to 10) satisfying the impact theory. Then as the r. d. is increased the shift grows somewhat quadratically from r. d. 10 to 24 as expected by statistical theory. Then a *second* nearly linear region prevails, from r. d. 24 to 40 (slope −1.66 cm^{-1}/r. d.). This second linear region is followed by a clear indication of curving up to weaker red shift, (turning back region). This may mean that as the r. d. is high a factor of repulsive electrostatic potential sets in, and increases as the r. d. is increased. This "red shift vs r. d. plot" is probably typical for all spectral lines in a foreign gas which produces a "mild" red shift.

The authors would like to extend the plot in Fig. 7 still further with reference to observations obtained from a ballistic compressor [7]. As the r. d. of the foreign gas is further increased beyond the turning back region, the red shift would continue to decrease giving a broad minimum on the plot. Then the curve would go up quite linearly passing the zero shift border to a violet shift. And then the violet shift would continue to increase very strongly as the r. d. further increases.

Probably all spectral lines will shift towards "violet" if the applied foreign gas pressure is sufficiently high. For cases where the red shifts are mild, such as those mentioned in Table 3 of reference [7], the required foreign gas pressure are easily attainable. For the cases where the red shift is very strong, such as in the case of Ca (1)/Ar, the Ar pressure required to produce a violet shift is enormously high.

The shift of Sr(1) at low densities of Ar (from 0.1 to 10 r. d.) was -0.27 cm^{-1}/r. d. at 474.8°C. Hindmarsh's shift for r. d.'s below 1 was -0.21 cm^{-1}/r. d. at 407°C. The corresponding result for Ca(1)/Ar was -0.23 cm^{-1}/r. d. at 556°C.

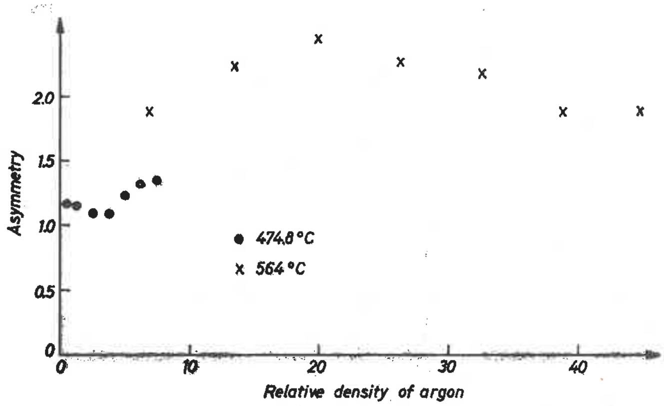

Fig. 8. The asymmetry of Sr(1) in argon

The asymmetry is measured by the ratio of the red half to the violet half of the line width at half intensity. In Fig. 8 is shown the asymmetry for Sr(1)/Ar. It lay between 1.0 to 1.4 from r. d. 0.4 to 7.4 (at 474.8°C) and between 1.8 to 2.5 from r. d. 6.7 to 44.7 (at 564°C). The asymmetry was higher for higher temperature.

C. Calculation of the physical constants from the observed data

All physical constants were derived on the basis of impact theory. Accordingly, the experimental values used must be those for which the r. d. were low and the values of shift and half-width changed linearly with r. d. If a frequency perturbation due a (6–12) potential is assumed and since perturber interactions were proven to be additive [8], the values of the difference of interaction constants ΔC_6 and ΔC_{12} can be found from the observed half-width and shift [9]. A three-point smooth-curve interpolation procedure [10] was used by Hindmarsh's table. The values of ΔC_6 and ΔC_{12} and other physical constants were found and listed in Table II. Fig. 9 is a plot of the Lennard-Jones difference potential for Sr(1)/Ar.

TABLE II

The physical constants computed from the experimental values of shift and half-width for Sr 4607/Ar

Shift, $\Delta\nu_m$	-0.27 cm^{-1}/r.d.	σ_r	2.95×10^{-14} cm^2
Half-width, $\Delta\nu_{\frac{1}{2}}$	0.64 cm^{-1}/r.d.	ϱ	9.69 Å
Temperature, T	474.8°C	r_m	10.91 Å
ΔC_6	9.67×10^{-31} cm^6/sec or 1.02×10^{-57} erg/cm^6	$\left(\frac{dV}{dr}\right)_{r_0}$	6.67 cm^{-1}/Å
ΔC_{12}	0.82×10^{-72} cm^{12}/sec or 0.86×10^{-99} erg/cm^{12}	$\left(\frac{d^2V}{dr^2}\right)_{r_m}$	0.92 cm^{-1}/(Å)^2

where σ_r is the real part of optical collision cross-section, ϱ — the optical collision radius, r_m — interatomic distance at which the potential is a minimum, $\left(\frac{dV}{dr}\right)_{r_0}$ — the slope of potential curves at $r = r_0$, r_0 being the interatomic distance at which the potential is zero, and $\left(\frac{d^2V}{dr^2}\right)_{r_m}$ — the curvature of potential curve at potential minimum, $r = r_m$.

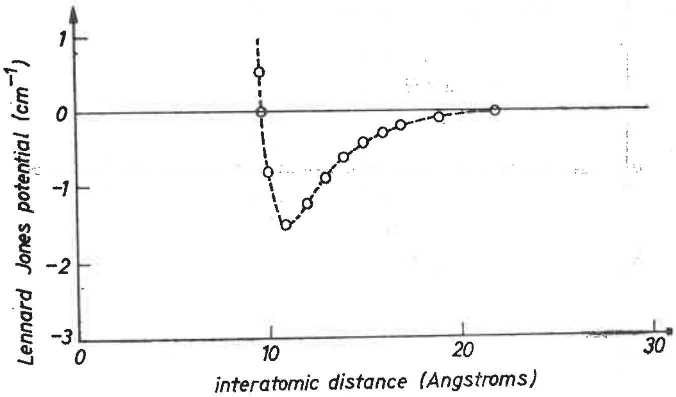

Fig. 9. A plot of Lennard-Jones difference potential derived from results tabulated in Table II

REFERENCES

[1] J. M. Farr, W. R. Hindmarsh, *J. Phys.* **B4**, 568 (1971).
[2] S. Y. Ch'en, A. T. Lonseth, *Phys. Rev.* **A3**, 946 (1971).
[3] H. Kuhn, *Philos. Mag.* **18**, 987 (1934).
[4] E.. Lindholm, *Ark. Mat. Astron. Fys.* **32A**, 17 (1945).
[5] P. W. Anderson, J. D. Talman, *Bell Telephone System*, Tech. Publ. No. 3117 (1956).
[6] H G. Kuhn, *Atomic Spectra*, Academic Press, New York 1969.
[7] P. L. Henry, S. Y. Ch'en, N. Sidell, *J. Quant. Spectrosc. Radiat. Transfer* **14**, 405 (1974).
[8] S. Y. Ch'en, R. O. Garrett, *Phys. Rev.* **A4**, 412 (1971); H. C. Jacobsen, *Phys. Rev.* **A5**, 989 (1972).
[9] S. Y. Ch'en, Proc. International Conf. on Applied Pumping and Atomic Line Shape, Warsaw, Poland 1969, p. 403; W. R. Hindmarsh, A. D. Petford, G. Smith, *Proc. R. Soc.* **A297**, 296 (1967).
[10] J. Mathews, R. L. Walker, *Math. Methods of Phys.*, W. A. Benjamin, 1964, p. 330.